Petroleum 2 (2016) 273–281

Contents lists available at ScienceDirect

Petroleum

journal homepage: www.keaipublishing.com/en/journals/petlm

Original article

Cross-flow analysis of injection wells in a multilayered reservoir

Mohammadreza Jalali [a, *], Jean-Michel Embry [b], Francesco Sanfilippo [c], Frederic J. Santarelli [c], Maurice B. Dusseault [d]

[a] Geological Institute, ETH Zurich, Zurich, Switzerland
[b] Baker Hughes, Aberdeen, United Kingdom
[c] Geomec Environmental Management AS, Stavanger, Norway
[d] Earth & Environmental Sciences Department, University of Waterloo, Waterloo, ON, Canada

ARTICLE INFO

Article history:
Received 3 March 2016
Received in revised form
23 May 2016
Accepted 25 May 2016

Keywords:
Cross-flow
Multilayered
Sandstone reservoir
Sand production
Skin factor

ABSTRACT

During fluid injection into a multilayered reservoir, a different pressure gradient is generated across the face of each permeable layer. This pressure gradient generates driving forces in the wellbore during well shut-in that causes the injected fluid moves from higher pressure layers to lower pressure layers, a phenomenon known as interwell cross-flow. Cross-flow behavior depends on the initial pressure in the permeable layers and may be referred to as natural cross-flow (identical or natural initial pressures) and forced cross-flow (different initial pressures because of exploitation). Cross-flow may induce sand production and liquefaction in the higher pressure layers as well as formation damage, filter cake build-up and permeability reduction in the lower pressure layers. Thus, understanding cross-flow during well shut-in is important from a production and reservoir engineering perspective, particularly in unconsolidated or poorly consolidated sandstone reservoirs.

Natural and forced cross-flow is modeled for some injection wells in an oil reservoir located at North Sea. The solution uses a transient implicit finite difference approach for multiple sand layers with different permeabilities separated by impermeable shale layers. Natural and forced cross-flow rates for each reservoir layer during shut-in are calculated and compared with different production logging tool (PLT) measurements. It appears that forced cross-flow is usually more prolonged and subject to a higher flow rate when compared with natural cross-flow, and is thus worthy of more detailed analysis.

1. Introduction

Multiple stacked/layer-cake type reservoir fields – e.g. Gulf of Mexico, Gulf of Guinea, North Sea, etc. – have sand layers hydraulically separated by more-or-less continuous shale layers with thicknesses from 1 to 100 m. Injection wells in such cases are commonly drilled and completed in multiple reservoir layers. During water injection into a depleted reservoir, different pressure gradients in various layers are generated where the controlling factors are the injection rate (Q^i) and the petrophysical properties for each layer – i.e. porosity (ϕ^i), permeability (k^i), exposed surface area of each layer (depends on the wellbore radius (r_w) and layer thickness (h^i)), total compressibility (c_t^i) and initial skin factor (s^i) where superscript i refers to the layer's number. There exist some other relevant parameters such as k_{ro} and k_{rw} during water injection, the permeability response of each layer to solids and oil entrained within the injected water over time as well as well trajectory, however, these parameters are not considered in the current study.

Induced differential pressures and gradients will begin to dissipate as soon as injection ceases, if zonal isolation mechanisms such as ICVs (in-flow control valves) are not present or

* Corresponding author. NO F27, Sonneggstrasse 5, 8092 Zurich, Switzerland. Tel.: +41 44 633 81 76.
E-mail address: jalalim@ethz.ch (M. Jalali).
Peer review under responsibility of Southwest Petroleum University.

Production and Hosting by Elsevier on behalf of KeAi

http://dx.doi.org/10.1016/j.petlm.2016.05.005

active. First, the pressure gradient in an individual layer generates fluid flux from the near-wellbore toward the far-field. However, pressure dissipation will also occur through the wellbore as during shut-in, the wellbore pressure decreases because of flux into the more permeable layers, and the pressure in the more permeable layers can soon become less than the pressure in other layers. Then, the layer with a pressure higher than the wellbore is producing fluid that flows through the well and enters the layers with lower pressure. This pressure equalization phenomenon is known as cross-flow (Fig. 1), and for clarity, two terms are introduced, which will be used throughout:

Natural cross-flow: This occurs when all the layers are at hydrostatic pressure equilibrium with each other under the no-flow condition. The pressure in each layer is $p^{i+1} = p^i + \rho_w g(z^{i+1} - z^i)$, where ρ_w is the density of the injected water, g is gravitational acceleration, and z^i is the vertical depth of layer i. The main drive mechanism for natural cross-flow is the difference of diffusivity ($D = k/\phi\mu_w c_t$) between layers (where k is the intrinsic permeability, ϕ is porosity μ_w is viscosity of water, c_t is the total reservoir compressibility). Note that this case does not preclude over-pressured or under-pressured cases, as it is the pressure and diffusivity differentials between layers that are important, not the absolute values.

Forced cross-flow: This occurs when the injected layers are not at pressure equilibrium because of injection/production activities – i.e. cases when there is a differential depletion or pressurization of different layers. The pressure difference between the layers is the main driving mechanism for forced cross-flow.

The flow duration is also different in these two cases; natural cross-flow occurs for a much more limited period of time until dissipation of the pressure gradient occurs, whereas forced cross-flow can be a major effect as long as significant induced pressure disequilibrium exists.

Cross-flow may cause sand production into the wellbore due to pressure drawdown, and this particulate material may also be carried into the lower-pressure layers with the flow of fluids. This will alter the well's injection response, and may lead to perforation plugging (sand accumulation in the well) or it may plug or damage downhole equipment such as ICDs (in-flow control devices) and ICVs, which control zonal injection. Under exceptional circumstances, interwell cross-flow can reach an initial rate of several thousand barrels per day, which can even affect the reservoir behavior beyond the immediate wellbore region [1]. These issues are most important in weak (high porosity) sandstone reservoirs; for example, Santarelli et al. [2] presented a field case from the Norwegian Sea where cross-flow and related sand production during shut-in led to massive injectivity losses and to the complete plugging of wells because of sand layer liquefaction.

Most cross-flow studies focus on interlayer cross-flow during production or injection, and notable work has been done by Russell and Prats [3] and Gao and Deans [4]. Modine et al. [5] implemented a superposition method to model cross-flow in a numerical simulator and they found this method to be reasonably accurate, straightforward, and cost-effective. Fedorov et al. [6] considered non-stationary operation of a well in a reservoir with two-layers of identical properties except for permeability, and studied the effect of shut-in on the wellbore including cross-flow behavior at the beginning of injection and also when the injection rate was changed.

This article seeks to address the following questions:

- Why do we want to model injection well cross-flow?
- How can we model cross-flow after shut-in?
- What field data are needed to model cross-flow?
- Can cross-flow modeling be quantitative?
- How can we use cross-flow modeling results?

To answer these questions, the effects of natural and forced cross-flow on the sanding potential of 13 water injectors (named as A-1 to A-7 and B-1 to B-6) in a North Sea oil field are reviewed and compared. The effect of skin factor on natural and forced cross-flow is studied. Also, the effect of cross-flow on sand production is described qualitatively and a pattern is suggested for understanding sanding in injector wells during shut-in periods.

There exists eight sand layers in the considered reservoir (named as LA-1 to LA-8) which are hydraulically separated by nine more-or-less continuous shale layers (named as SH-1 to SH-9). Fig. 2 schematically depicts the sand layers which were

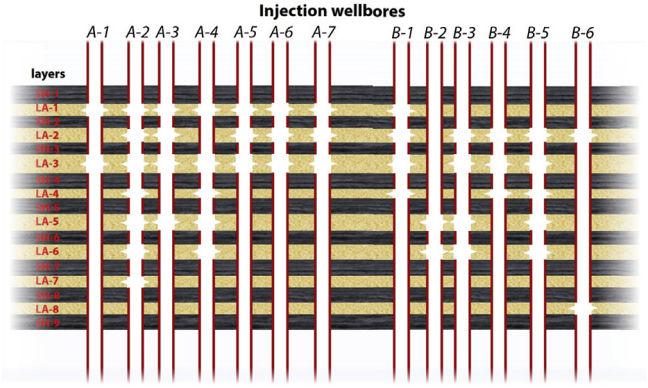

Fig. 2. Schematic representation of the perforated intervals in each injection well in the considered oil field.

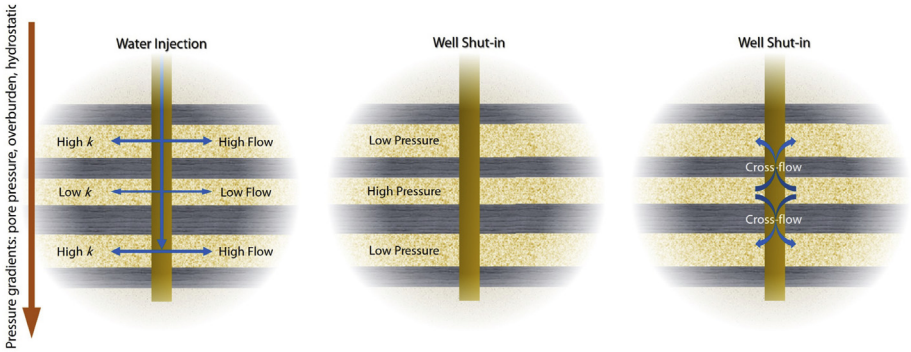

Fig. 1. Schematic representation of interwell cross-flow in a multilayered reservoir.

perforated in each injection well. Throughout this paper, a positive flow rate corresponds to injection (*out-flow* from well) and a negative flow rate corresponds to production (*in-flow* to well).

2. Natural cross-flow

Natural cross-flow in an injector in a series of sand layers separated by shale intervals (i.e. where interlayer cross-flow is negligible) at pressure equilibrium is controlled by the difference of diffusivity between layers, the amount of injected fluid and the duration of the injection period.

The approximate distance between the injection and production well rows in the field case studied is roughly 1700 m, which is assumed to be the model drainage radius (external boundary). The field has experienced different injection and shut-in sequences during its life, but only one of the injection events is simulated in this study – a 48-hour injection period at a rate of 35,000 bpd followed by a shut-in of another 48 h.

Consider an axisymmetric injection well with a constant total flow rate (Q_t) and a fixed external pressure (p_{out}) at the outer boundary to simulate the presence of surrounding producers. Fluid rate into each layer during injection is proportional to the permeability-thickness product (kh) – i.e. $Q^i = (k^i h^i / \sum k^i h^i) Q_t$ – where the skin effect around the wellbore is neglected for now. The choice of injection and shut-in duration is based on the following criteria:

- Injection is sufficient to reach a steady-state condition at the end of the injection period for most of the layers.
- The shut-in period is long enough to let natural cross-flow essentially dissipate.

Total reservoir compressibility is taken equal to $c_t = 4.5 \times 10^{-5}$ bar^{-1} (3.1×10^{-6} psi^{-1}), the compressibility of water (i.e. the effect of pore compressibility is neglected). A value of 0.315 cP is chosen for reservoir water viscosity, a reasonable assumption for early injection periods when the cooled zone around the injector is small compared with the overall dimensions of the model.

The other petrophysical parameters around one of the injection wells (well B-3), estimated from the CPI (computer processed interpretation) log and well geometry, are listed in Table 1. An arithmetic average is used for the porosity and permeability estimates, and only one isotropic value for permeability is used for each layer in this study (i.e. $k_v = k_h$).

In order to model the interwell cross-flow, it is required to simulate both injection and shut-in phases. For the injection part, the mass conservation equations for each layer in a radial coordinate is considered under a constant injection rate boundary condition. Total injection rate into each borehole is divided into each layer based on the transmissibility of each layer during the injection phase. During the shut-in phase, injection rate into the borehole is assumed to be zero. A transient implicit finite difference approach is implemented to solve the mass conservation governing equations. For this purpose, each layer is discretized via an irregular (logarithmic spacing) point-distributed grid, such that the first grid point in each layer corresponds to the wellbore. More information on the model specifications and assumptions can be found in Jalali et al. [7]. The model is run with above mentioned parameters to simulate natural cross-flow of the well B-3. Wellbore pressure during 48 h of injection into well B-3 with a rate of 35,000 bpd followed by a 48-hour wellbore shut-in is shown in Fig. 3. It should be mentioned here that the effect of skin factor in this part is not considered.

Table 1
Petrophysical properties of perforated sand layers LA-2, LA-3, LA-5 and LA-6 around the well B-3.

Properties	Layer name			
	LA-2	LA-3	LA-5	LA-6
Effective porosity (–)	0.11	0.30	0.11	0.18
Permeability (mD)	182	2626	337	1010
Height (ft)	18	37	77	31

Based on Fig. 3, pressure increases suddenly after the injection starts and a steady-state condition is reached after roughly 16 h. When the well is shut-in, the pressure falls for a similar time until a condition of $p_0 = 4415$ psi is reached. This pressure profile is not a good representation of field conditions as a zero skin factor was assumed for the well B-3; in fact, the calculated pressure is expected to be less than the field pressure because of a positive skin factor around the wellbore. In Fig. 3, for example, the pressure difference required to inject at 35,000 bpd into well B-3 is only about 98 psi, significantly less than the upper limit of estimation, which is on the order of 1600–1800 psi.

2.1. Skin factor effect

The effect of skin factor is considered in the mathematical model via introduction of the near-well permeability modifier (S^i); this coefficient is roughly equivalent to the zero-thickness conventional skin coefficient (i.e. a zero-thickness impedance term). An identical well permeability modifier is used for each layer in the simulation – i.e. $S = S^i = S^{i+1}$ – because of an absence of appropriate field data to further constrain the input data. Step-rate test data are used to estimate the value of the near well permeability modifier in well B-3 (Fig. 4).

The matrix injection pressure at a rate of 25,000 bpd is estimated either directly or by an extrapolation process similar to that shown in Fig. 4. The rate of 25,000 bpd is selected to be significantly above the minimum range of accuracy of the flowmeters. The model is run to simulate an injection sequence at 25,000 bpd for a period of 10 h and then near-well permeability is adjusted via calibration so that the pressure after 10 h is equal to the pressure determined from the step-rate test. Fig. 5 below shows the calibrated model for well B-3.

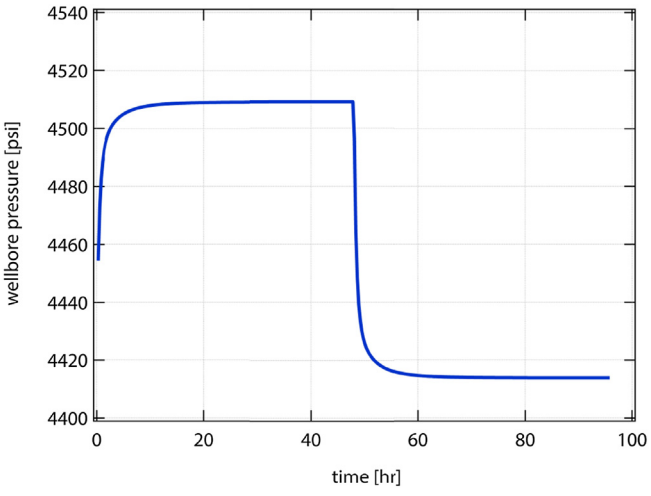

Fig. 3. Evolution of wellbore pressure during the simulation of the natural cross-flow on well B-3.

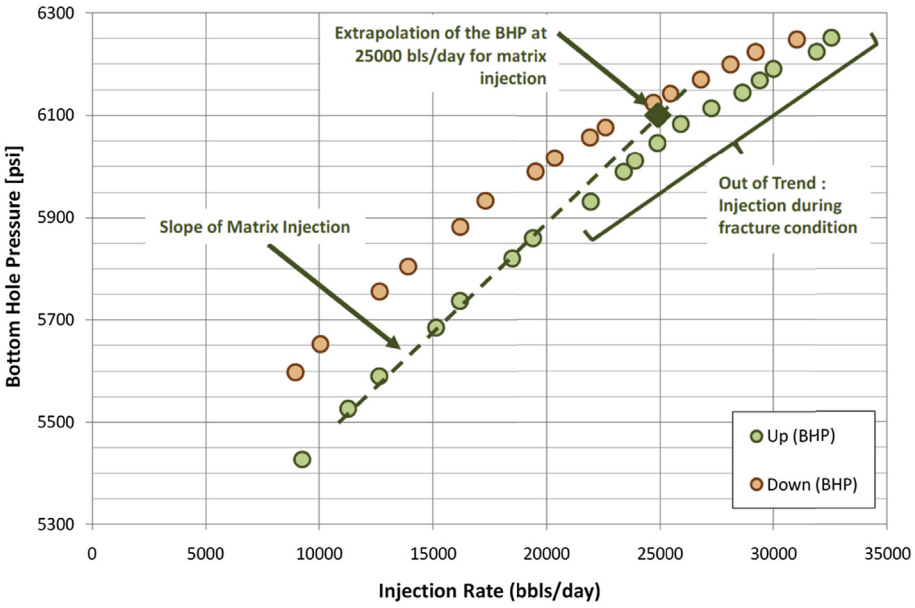

Fig. 4. Step-rate test performed on well B-3.

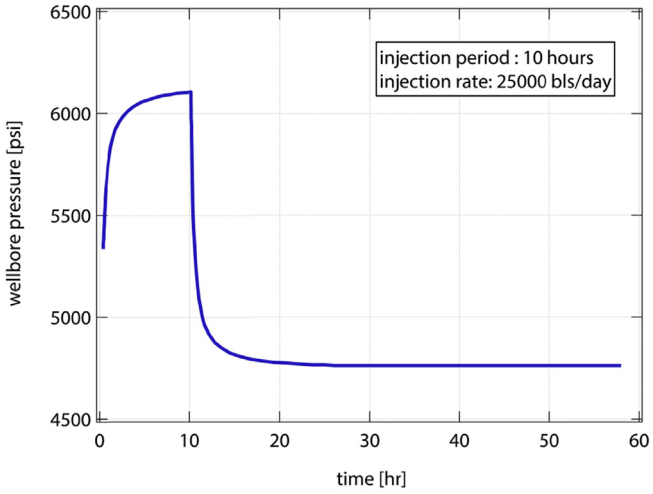

Fig. 5. Calibrated injection pressure at 25,000 bpd in Well B-3.

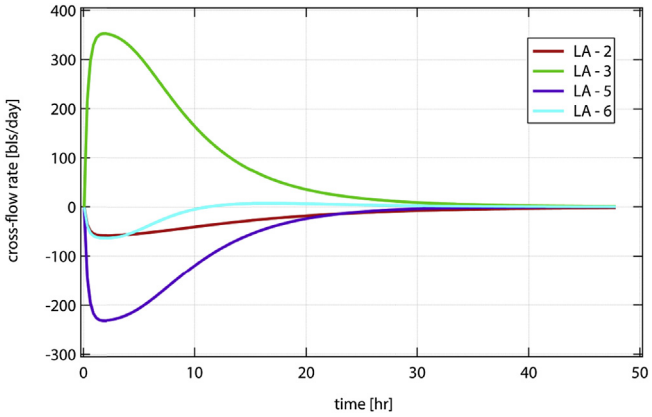

Fig. 6. Cross-flow results for well B-3 (natural cross-flow simulation).

Using this procedure, the near-well permeability modifier (S) for well B-3 is estimated to be 20. The matrix injection pressure at 25,000 bpd rate is about 6000 psi and the reservoir pressure is approximately 4760 psi, determined from Horner analysis of the step-rate test data. Similar procedure is conducted for all the 13 injectors in the field and the results show a large near well permeability modifier with a range from 8.5 up to 42, which indicates large positive skins for all the considered wells. This fact is in agreement with the well test analyses were done in each well.

2.2. Natural cross-flow simulation results

The calibrated model using the near well permeability modifier ($S = 20$) is executed for well B-3 for a 48-hour injection period at 35,000 bpd, followed by a 48-hour closure. The flow rates into each layer ($Q > 0$) and from each layer ($Q < 0$) after the shut-in are plotted in Fig. 6. This Figure demonstrates that the permeability-thickness product (kh in Table 2) is the key parameter for quantifying natural cross-flow.

Layer LA-3 has the highest kh which corresponds to the dominant layer for injection, and during cross-flow, well B-3 produces from layers LA-2, LA-5, and LA-6, all with kh values substantially less than layer LA-3. This behavior – i.e. production from low kh layers with flow into the one with the highest kh – frequently happens in the case of natural cross-flow, although exceptions do occur.

The maximum flow rate for each layer is reached about 2 h after the well has been shut-in. This time is identical for all the layers and it is essentially controlled by the distance between the

Table 2
Permeability-thickness and maximum flow rate for perforated layers around well B-3 during natural cross-flow.

Properties	Layer name			
	LA-2	LA-3	LA-5	LA-6
Permeability-thickness (mD ft)	3276	97,169	25,945	31,323
Maximum flow rate (bpd)	−57.97	352.78	−231.72	−63.10

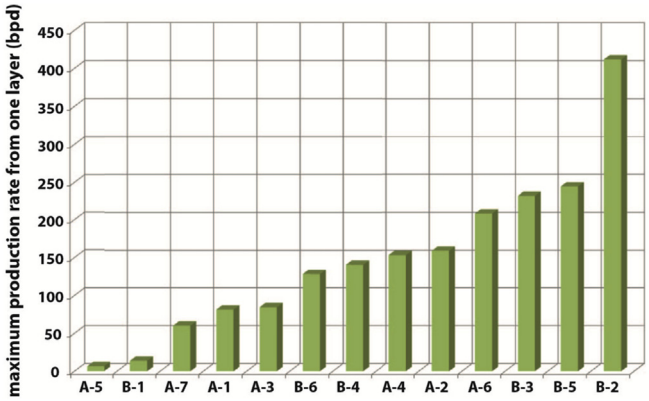

Fig. 7. Maximum rate for the layer with maximum production rate for each 13 injectors.

well and the external boundary of the model, and by the permeability contrast between the layers – i.e. by the time taken for pressure to dissipate in the high permeability layer, by transferring fluids towards the external boundary of the model. The behavior of layer LA-6 is different than the other three layers, i.e. it experiences in-flow during early shut-in for about 11 h, and then experiences minor out-flow for the rest of the simulated time.

This simulation is repeated for all 13 wells in the field. The maximum simulated flow rates during natural cross-flow are relatively modest, a maximum of 412 bpd in well B-2. Note that maximum flow rates are almost identical to those obtained with a permeability modifier of 1 (i.e. a well without skin), which means that the presence of a realistic skin effect does not seem to significantly affect the natural cross-flow behavior of a well. Fig. 7 plots the maximum flow rate from the layer with maximum in-flow during natural cross-flow for each injector of the field; the median value for this maximum production rate is 141 bpd and the arithmetic average is 148 bpd. This plot presents the importance of natural cross-flow during the shut-in phase of injectors in the considered field.

3. Forced cross-flow

Forced cross-flow refers to cases in which the different layers perforated on an injector are not at pressure equilibrium, so the pressure difference between the layers now becomes the main driving force behind cross-flow. The initial pressure of each layer, a vital piece of data for simulation, is estimated via MDT logging (Modular Formation Dynamics Tester[1]). The MDT has been used frequently in this field and provided a direct measurement, but unfortunately for a limited period of time only. Other model parameters are the same as for the natural cross-flow case simulations, including the value of the near-well permeability modifier. Table 3 summarizes the measured pressure via MDT logging which is used for the modeling of forced cross-flow in well B-5.

The flow behavior during forced cross-flow is quite complex (Fig. 8) as the direction of cross-flow changes over time. Layer LA-5, for example, shows in-flow for a short period directly after shut-in (i.e. negative flow rate in Fig. 8) but ends up in an out-

[1] This is a Schlumberger Trademark name; its use or the use of any other trademark in this article does not imply an opinion of the authors and is not to be construed as an endorsement.

Table 3
Reservoir pressure derived from MDT measurements and maximum flow rate for perforated layers around well B-5 during the forced cross-flow.

Properties	Layer name				
	LA-2	LA-3	LA-4	LA-5	LA-6
Pressure (psi)	4880.59	4880.59	4880.59	4870.52	4870.52
Maximum flow rate (bpd)	−23.85	−44.53	−5.43	30.04	43.63

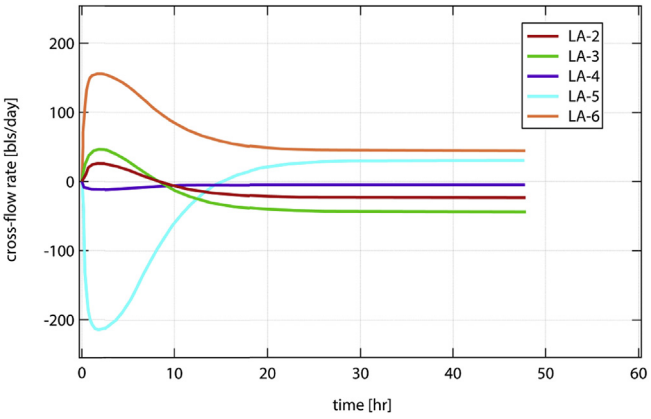

Fig. 8. Forced cross-flow response in the case of well B-5.

flow condition after about 14 h (positive flow rate). In contrast, layers LA-2 (red) and LA-3 (green) start with out-flow, but end up evidencing in-flow after about 8 h.

This complex behavior for forced cross-flow may be interpreted as following. Initially the well is dominated by natural cross-flow but after some time the pressure gradients from the injection period are dissipated and replaced by the pressure differences among layers. The two drive mechanisms – i.e. pressure gradients due to injection for natural cross-flow; and reservoir pressure differences for forced cross-flow – are independent of each other, which explains the behavior shown in Fig. 8.

The maximum production rate of seven wells in the field during forced cross-flow is shown in Fig. 9. Compared to the natural cross-flow (Fig. 7), the production rate is greater during forced cross-flow for some wells (A-3, A-4, A-5). Forced cross-flow is strongly affected by the near-well permeability modifier and would have been significantly increased if a value of $S = 1$ had been used. For example, in the case of well A-4, the

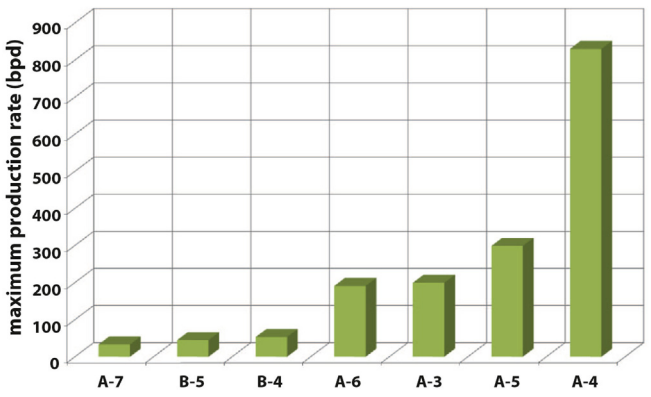

Fig. 9. Maximum production rate during forced cross-flow.

maximum production rate would have approached 40,000 bpd. This is in strong contrast with natural cross-flow where the near-well permeability has little effect on the flow rates.

4. Calibration of well B-3

The cross-flow modeling results obtained during this study are essentially semi-quantitative for a variety of reasons:

- Permeabilities derived from logs are used; these could not be confirmed by well test data at that time.
- MDT pressures are used for the forced cross-flow when they are available; these are only valid for a limited period of time after injection into the well begins, or it is assumed that all layers are at pressure equilibrium (natural cross-flow).

As a consequence, the cross-flow model needs to be calibrated with field data to give fully quantitative results. Calibration is performed for well B-3 for which PLT data are available for the well completion date, as well as for three years later in the well's life. Table 4 shows the flow distribution recorded during the two PLT logs performed on well B-3. It clearly shows significantly different flow allocation during the two PLT measurements for the following reasons:

- The first PLT was conducted in conditions of matrix injection while the second one was conducted in conditions of fracture injection (hydraulic fractures generated during injection by thermoelastic contraction). This difference was shown in the results of the step rate test on Fig. 4 by slope changes in the relationship between injection rate and bottom-hole pressure.
- The first PLT was conducted immediately after well completion (i.e. before any significant sanding occurred), whereas the second was conducted much later when the well behavior could have been affected by various phenomena such as partial filling of some perforation tunnels, removal of wellbore skin as a result of sand production, and improvement of near-well permeability to water.

The flow condition for the first PLT is modeled and then the calculated downhole pressure is matched with the PLT pressure using a permeability modifier of $S = 12.7$ instead of the value of $S = 20$ used to match the flow during the step-rate test (Fig. 4). This indicates a degradation of the near-well permeability during the three years separating the two estimates for S; which is a result of sanding within the wellbore.

In the case of the second PLT, a logging pass was performed with the wellbore shut-in and cross-flow was detected from lower formations towards the upper ones (Table 5). The cross-flow was measured roughly 2 h after shut-in following the low pass of the PLT – i.e. approximately 6.5 h of injection at 15,000 bpd – and the high pass of the PLT – i.e. 10 h of injection at 28,000 bpd.

Table 4
Flow distribution during the two PLT logs performed on well B-3.

Layer name	PLT after completion		PLT 3 years after completion	
	Flow rate (bpd)	Percentage (%)	Flow rate (bpd)	Percentage (%)
LA-2	23.1	0.9	1489.3	5.2
SH-3, LA-3	1912.7	74.6	12344.3	43.1
SH-4, SH-5, LA-5, LA-6	625.6	24.4	14807.4	51.7
SH-7	0.0	0.0	0.0	0.0
Total	**125.75**	**100.0**	**28,641**	**100.0**

Table 5
Cross-flow recorded during the shut-in pass of second PLT on wellbore B-3.

Zone name	Layer name	Flow rate (bpd)
Zone 1	LA-2	90.00
Zone 2	SH-3	277.70
Zone 3	LA-3	29.90
Zone 4	SH-5, LA-5	−69.40
Zone 5	SH-6, LA-6	−324.30
Zone 6	SH-7	0.00

The PLT results are reproduced with the cross-flow model by rearranging the layers. This is done by grouping [zones 2 and 3] and [zones 4 and 5] into single zones (zones 23 and 45, respectively). Three different simulations (Run I, II, and III) are then performed:

- *RUN I* is performed using the permeability values from the CPI log alone. As shown in Table 6, the model results do not match the measured values. A possible explanation for this relatively poor match is that the CPI permeability is the result of an interpretation and not a direct measurement.
- *RUN II* is simulated using the first PLT performed on well B-3 after completion to modify the *kh* partitioning between layers according to the flow partitioning of Table 5, while keeping the total *kh* of the well to its CPI value. The idea here is that the initial PLT on well B-3 was performed under matrix injection and was representative of the real *kh* of the sand formations. The results of this simulation are shown in Table 6, which are quite close to the measurements, especially for zone 45.
- *RUN III* in Table 6 corresponds to a second modification of *kh* partitioning but this time using the in-flow profile from the second PLT which was done three years after completion at a rate of 28,000 bpd. The results from the third run are a poor match to the cross-flow measured during the shut-in pass of the PLT.

The cross-flow measured during the shut-in pass of the PLT test on well B-3 after completion can be simulated reasonably well with the cross-flow model (i.e. *RUN II*), and it is noted that the match is achieved without the use of any mathematical calibration factor. It simply requires an adjustment of the *kh* partitioning based on actual matrix flow – i.e. obtained from the data of the first PLT on the wellbore after completion – and an adjustment of the number of layers in the model – i.e. obtained from the shut-in measurement during the second PLT three years after the well completion.

5. Cross-flow and sand production

For the field studied; simulations of natural and forced cross-flow are performed for those wells where MDT logs are

Table 6
Simulation of the cross-flow recorded during the PLT performed three years after completion on well B-3.

Zone name	Measured flow rate (bpd)	Calculated flow rate (bpd)		
		RUN I	*RUN II*	*RUN III*
Zone 1	90	−23.9	−21.1	−49.7
Zone 23	307.6	245.7	385.7	96.9
Zone 45	−393.7	−293.8	−364.6	−47.2
Zone 6	0.0	−28.1	0.0	0.0

available (seven wells out of 13) and showed considerable depletion differences. Based on the results depicted in Table 7, forced cross-flow rates are often significantly larger than natural cross-flow rates – in excess of one order of magnitude larger (well A-5 for example). The flow direction during natural and forced cross-flow coincides in only three cases out of the seven (wells A-3, A-5, and A-6); the different mechanisms for natural and forced cross-flow explain this difference in flow direction.

Table 8 shows the forced cross-flow rates for wells where MDTs are available (seven wells out of 13), and natural cross-flow rates for other wells (six wells out of 13). Based on Table 8, only 8 out of 47 layers (17% of cases) are both weak (i.e. high sanding potential) and in production (in-flow) conditions during cross-flow. These layers are shown in pink; dark pink corresponds to layers with a complete failure condition prediction, light pink corresponds to layers where only a limited portion could be construed to have entered a failure condition. The classical

Table 7
Comparison of the forced and natural cross-flow for some of the wells in the studied field.

wellbore name (cross-flow type)	maximum flow rate (bbl/day)							
	LA-1	LA-2	LA-3	LA-4	LA-5	LA-6	LA-7	LA-8
A-3 (natural)	-55.10	-8.91	-84.38	---	148.54	---	---	---
A-3 (forced)	-139.18	-145.57	-199.26	---	484.11	---	---	---
A-4 (natural)	102.95	---	151.56	-66.72	-153.98	-33.96	---	---
A-4 (forced)	-830.10	---	521.70	8.60	20.53	279.27	---	---
A-5 (natural)	3.02	3.47	-6.49	---	---	---	---	---
A-5 (forced)	125.75	172.99	-298.74	---	---	---	---	---
A-6 (natural)	-15.25	208.47	-193.22	---	---	---	---	---
A-6 (forced)	-15.40	206.36	-190.96	---	---	---	---	---
A-7 (natural)	-4.08	60.08	-56.00	---	---	---	---	---
A-7 (forced)	-32.91	-13.59	46.34	---	---	---	---	---
B-4 (natural)	---	101.74	-141.14	39.40	---	---	---	---
B-4 (forced)	---	-53.14	41.06	11.93	---	---	---	---
B-5 (natural)	---	49.36	90.12	-6.94	-244.09	111.41	---	---
B-5 (forced)	---	-23.85	-44.53	-5.43	30.04	43.63	---	---

injection	< 100 bpd	< 500 bpd	> 500 bpd	production	< 100 bpd	< 500 bpd	> 500 bpd

Table 8
Possible sand producing layers during cross-flow.

wellbore name (cross-flow type)	maximum flow rate (bbl/day)							
	LA-1	LA-2	LA-3	LA-4	LA-5	LA-6	LA-7	LA-8
A-1 (natural)	-81.21	---	81.21	---	---	---	---	---
A-2 (natural)	-40.76	-37.44	99.48	159.65	-158.81	-14.94	-7.25	---
A-3 (forced)	-139.18	-145.67	-199.26	---	484.11	---	---	---
A-4 (forced)	-830.10	---	521.70	8.60	20.53	279.27	---	---
A-5 (forced)	125.75	172.99	-298.74	---	---	---	---	---
A-6 (forced)	-15.40	206.36	-190.96	---	---	---	---	---
A-7 (forced)	-32.91	-13.59	46.34	---	---	---	---	---
B-1 (natural)	9.51	12.68	-13.74	-8.45	---	---	---	---
B-2 (natural)	---	---	---	---	-411.81	411.81	---	---
B-3 (natural)	---	-57.97	352.78	---	-231.72	-63.10	---	---
B-4 (forced)	---	48.61	-100.08	51.32	---	---	---	---
B-5 (forced)	---	25.51	45.59	-12.23	-213.90	155.03	---	---
B-6 (natural)	---	128.31	---	---	---	---	---	-128.31

injectivity index	increase	decrease

failure condition	limited	complete

approach of sand strength and near well stress estimation is used and then their values are inserted in a field calibrated failure criterion [8].

Three wells (A-4, B-1, and B-3) in Table 8 experienced a strong decrease of injectivity index during their injection life, these are shown in red, and all contain weak layers experiencing in-flow during shut-in. Although well A-1 showed a large injectivity decrease, it does not contain a weak layer combined with in-flow during shut-in. Injectivity was increased in two wells, shown in a green color in Table 8. Well A-3 does not have any weak producing layers during cross-flow, whereas well A-2 has a weak layer (LA-6) with high sanding potential.

Based on the observed information, there appears to be a strong correlation between the occurrence of sanding during cross-flow (i.e. the presence of weak producing layers) and a reduction in injectivity of the wells, with the exception of wells A-1 and A-2. This suggests that there may be other mechanisms apart from cross-flow to explain the sanding behavior of these specific water injectors, despite the fact that cross-flow explains the majority of the injectivity changes that have been observed and analyzed so far. Santarelli et al. [9] suggested two other sanding mechanisms using field data analysis, direct downhole measurements and numerical modeling which are swabbing effect due to water-hammer effect and surface-flow between wells.

A down-hole camera survey was performed in well B-3 to observe the presence of sand along the injection tubing (Fig. 10). Snapshots "*ID1*" and "*ID2*" are full of debris whereas snapshot "*clean*" was taken from a clean interval for comparison.

Based on the second PLT data and *RUN III* results, the *ID2* snapshot was taken from zone 45, an in-flow zone, and it shows lots of debris in front of the perforations as a result of sand production during cross-flow (Tables 6 and 8). On the other hand, snapshot *ID1* is located in zone 23, an out-flow zone at a higher elevation than zone 45. Because of the cross-flow direction (from bottom to top) some amount of debris moved upwards to the sand face of zone 23 and blocked the perforations, which appears to be the case here, and heavier debris fell down due to gravity and filled the rathole, as shown in Fig. 11.

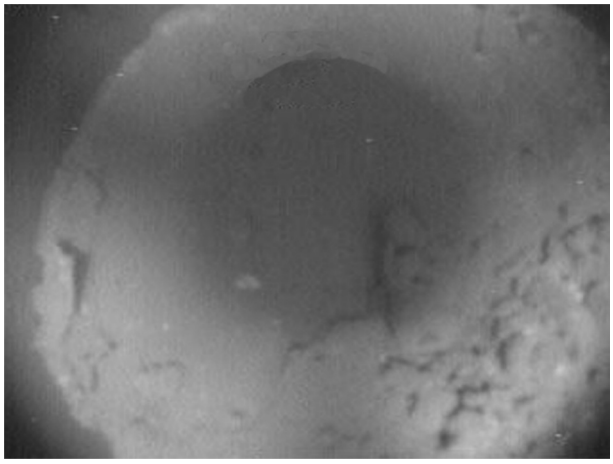

Fig. 11. Camera survey in well B-3: picture of the rathole filled with debris.

6. Conclusions

When an injector is shut-in, cross-flow between perforated intervals may occur which can induce sand production and liquefaction in the higher pressure layers and formation damage and permeability reduction in the lower pressure layers. Understanding and modeling cross-flow during well shut-in is important from a production and reservoir engineering perspective, particularly in unconsolidated or poorly consolidated sandstone reservoirs. This modeling can be done by considering the two different types of cross-flow, natural cross-flow and forced cross-flow:

(1) During natural cross-flow, all the perforated intervals are at pressure equilibrium and cross-flow occurs because different layers drain at different rates as the result of diffusivity differences (the effect of permeability difference is dominant). This leads to near-well pressure differences that drive the cross-flow.

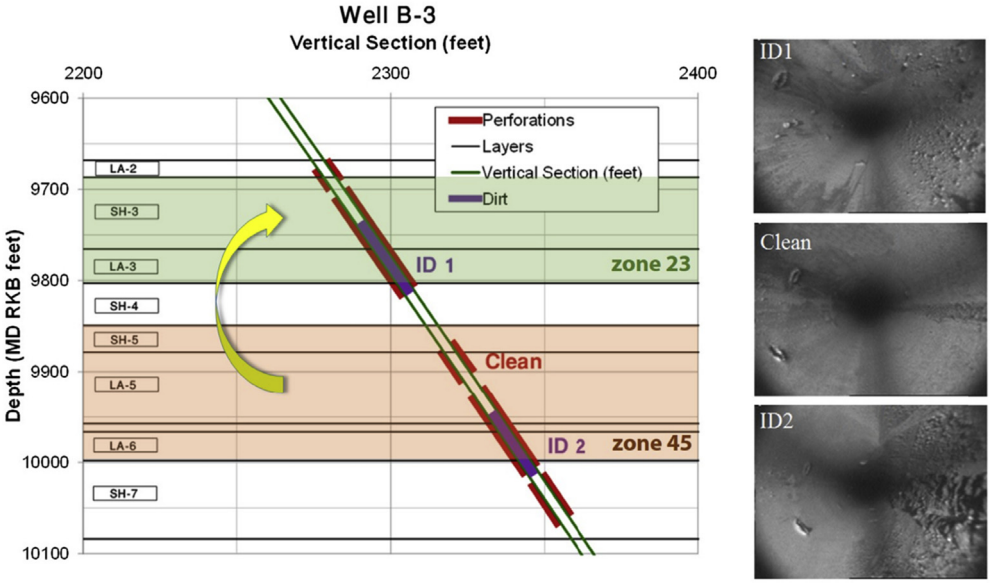

Fig. 10. Well B-3 trajectory with the pictures taken from the camera survey. Cross flow direction is from zone 45 (bottom) to zone 23 (top).

(2) During forced cross-flow, the perforated intervals are not at pressure equilibrium and the cross-flow happens because of pressure-head differences between layers.

It should be noted that natural cross-flow dies out after a few hours after the shutting in of the well, while forced cross-flow can last for days, or as long as pressure disequilibrium persists. The flow pattern during forced cross-flow can be complex when the beginning of the flow is governed by natural cross-flow, then followed by forced cross-flow. As the two cross-flow mechanisms are independent, this could lead to situations where a layer would show well in-flow from natural cross-flow before changing to well out-flow because of forced cross-flow. Though it is possible that the opposite sequence may also occur.

In this study, cross-flow in injectors of a North Sea oil field was studied. Combinations of field data were used to estimate the input parameters of cross-flow as well as for model calibration and quantification. For example, MDT log results were used to assess differential depletion in order to establish the existence of pressure disequilibrium and pressure-head differences leading to forced cross-flow.

Although a valuable combination of data such as PLT results, global well behavior, collapsed well data and camera survey data have been used to calibrate the model, the cross-flow study still is not fully quantitative because of various uncertainties. Some of the questions that should be answered to further quantify such studies are how the skin factor of each layer varies with time during cross-flow and how pressure behaves after MDT measurements. Still, there will be limitations in data collection even in a top-class field case like the one analyzed herein. This means that despite all reasonable attempts, cross-flow sanding potential studies will remain as a semi-quantitative process requiring experienced interpretation. Nevertheless, as we have shown, careful analysis greatly constrains the possible interpretations, allowing good engineering decisions to be made.

Nomenclature

c	compressibility (Pa^{-1})
D	fluid diffusivity (m^2/s)
g	gravitational acceleration (m/s^2)
h	formation thickness (m)
k	intrinsic permeability (m^2)
p	pressure (Pa)
Q	flow rate (m^3/s)
S	near well permeability modifier
z	vertical depth (m)
ϕ	porosity
μ_w	water viscosity (Pa s)
ρ_w	water density (kg/m^3)

SI metric conversion factors

bbl	$\times$1.59E-01 = m^3
bar	$\times$1.0E-01 = MPa
psi	$\times$6.895E-03 = MPa
cP	$\times$1.0E-03 = Pa.s
mD	$\times$9.869E-16 = m^2
ft	$\times$3.048E-01 = m

Abbreviation list

CPI	computer processed interpretation
ICD	in-flow control device
ICV	in-flow control valve
MDT	modular formation dynamics tester
PLT	production logging tool
mD	$\times$9.869E-16 = m^2
ft	$\times$3.048E-01 = m

References

[1] J. Bellarby, Well Completion Design, First ed., Elsevier, Amsterdam, 2009.
[2] F.J. Santarelli, E. Skomedal, P. Markestad, H. Berge, H. Nasvig, Sand production on water injectors: just how bad can it get? SPE Drill. Complet. 15 (2) (2000) 132–139.
[3] D. Russell, M. Prats, Performance of layered reservoirs with crossflow - single-compressible-fluid case, SPE J. 2 (1) (1962) 53–67.
[4] C. Gao, H. Deans, Pressure transients and crossflow caused by diffusivities in multilayer reservoirs, SPE Form. Eval. 3 (2) (1998) 438–448.
[5] A. Modine, K. Coats, M. Wells, A superposition method for representing wellbore crossflow in reservoir simulation, SPE Reserv. Eng. 7 (3) (1992) 335–342.
[6] K. Fedorov, L. Kadochnikova, S. Repetov, Analysis of wellbore crossflows for nonstationary operation of a well in an inhomogeneous multilayer bed, J. Appl. Mech. Tech. Phys. 42 (3) (2001) 455–459.
[7] M.R. Jalali, J.M. Embry, F.J. Santarelli, M.B. Dusseault, Natural cross-flow rate modeling in complex reservoirs, in: 72nd EAGE Conference & Exhibition. Barcelona, Spain, 2010.
[8] J. Tronvoll, M.B. Dusseault, F. Sanfilippo, F.J. Santarelli, The tools of sand management, in: Proceeding of the SPE Annual Technical Conference and Exhibition, New Orleans, Louisiana, 2001.
[9] F.J. Santarelli, F. Sanfilippo, J.M. Embry, M. White, J. Tumbull, The sanding mechanisms of water injectors and their quantification in terms of sand production: example of the buzzard field (UKCS), in: Proceeding of the SPE Annual Technical Conference and Exhibition, Denver, Colorado, 2011.